ELSEVIER

Journal of Luminescence 64 (1995) 283–290

JOURNAL OF LUMINESCENCE

Femtosecond time-and-space domain holograms: diffraction on the edge of time

Alexander Rebane*, Olavi Ollikainen[1], Heinrich Schwoerer, Daniel Erni, Urs P. Wild

Laboratory of Physical Chemistry, Swiss Federal Institute of Technology, ETH-Zentrum, Zürich, Switzerland

Received 13 October 1994; revised 24 November 1994; accepted 17 December 1994

Abstract

We study the diffraction properties of time-and-space domain holograms stored with femtosecond light pulses with a coherence length much smaller than the lateral geometrical dimension of the hole-burning sample. We show that one can observe diffraction of read out beam on the virtual 'time edge' separating the spatial regions where the delay between the reference and the object pulses is either positive or negative. We also demonstrate that by placing a Fourier-transforming lens in the beam diffracted from the 'time edge' a spatial intensity pattern proportional to the homogeneous hole-burning spectrum is observed.

1. Introduction

Time-and-space domain holography [1–3] can be viewed upon as a more general case of conventional holographic process, in which the recording media remembers, in addition to the spatial picture, also the spectral intensity of the illuminating light. The time resolution is in this case Fourier-related to the spectral properties of the recording media: the shortest time that can be reproduced is approximately given by the inverse value of the frequency width of the inhomogeneous absorption band, while the largest time interval that can be coherently recalled from the hologram is given by the inverse value of the homogeneous line width of the molecules. It has been demonstrated that recording of full scenes of subpicosecond events is possible by using organic dye-polymer photochemical spectral hole-burning (SHB) materials which have very broad inhomogeneous bands [4, 5].

Another special property of time- and space domain holograms is that they preserve the information about the arrow of time: if the zero point on the time axis is established by applying a very short reference pulse, then the amplitude of the object, which belongs to the times later than zero will create a hologram with a different direction of diffraction as compared to the hologram created by the object arriving at times before zero. Such asymmetry of diffraction is directly related to the physical causality principle [6] was applied in [7] for imaging of objects hidden behind a strongly scattering screen.

If we are using very short (subpicosecond) pulses to record time-and-space domain holograms, then a situation may occur when the lateral spatial

* Corresponding author.

[1] Permanent address: Institute of Physics of the Estonian Academy of Sciences, Riia Street 142, EE2400 Tartu, Estonia.

SSDI 0022-2313(95)00043-7

dimensions of the sample exceed the coherence length of the light by more than hundred times. Then it is possible that one spatial region of the hologram cross-section represents the time after zero, while the other spatial region of the same hologram image belongs to the time before zero. Consequently, at the line between the two regions where the sign of the time delay changes the diffraction direction of the hologram will suffer an abrupt jump.

In the present paper we study the diffraction properties of femtosecond time-and-space domain holograms which contains such causality-related abrupt features and show that we can use this virtual 'time edge' to observe the homogeneous line shape of the hole-burning molecules.

2. Theoretical considerations

The diffraction properties of time-and-space domain holograms were previously treated in Refs. [2,6] by assuming that the time delay between the reference and the object pulse is either positive or negative over the whole area of the hole-burning sample. Here we are considering the opposite situation, where the sign of the delay is positive in one half of the hologram plane, while in the other half of the hologram the delay is negative. Our goal is to find an expression for the spatial distribution of the intensity of the diffracted light in the first positive (or in the first negative) diffraction order measured in the focal plane of a lens which is performing spatial Fourier transformation.

Let a thin plate of SHB material positioned in the $z = 0$ plane be illuminated at normal incidence angle with a plane wave reference pulse with amplitude,

$$A_{\mathrm{ref}}(t, z) = p\left(t - \frac{z}{c}\right) \mathrm{e}^{\mathrm{i}2\pi\nu_0\left(t - \frac{z}{c}\right)}, \tag{1}$$

where $p(t)$ is the time domain envelope of the pulse, ν_0 is the carrier frequency and c is speed of light. An object pulse with the same envelope function is applied at an angle α with respect to the z-axis (see Fig. 1(a), and is described by amplitude,

$$A_{\mathrm{obj}}(t, z, y) = p\left(t - \frac{z\cos\alpha - y\sin\alpha}{c} - \tau_0\right) \times \mathrm{e}^{\mathrm{i}2\pi\nu_0\left(t - \frac{z\cos\alpha - y\sin\alpha}{c} - \tau_0\right)}, \tag{2}$$

where τ_0 is the delay between the reference and the object wave fronts at the origin of the coordinates.

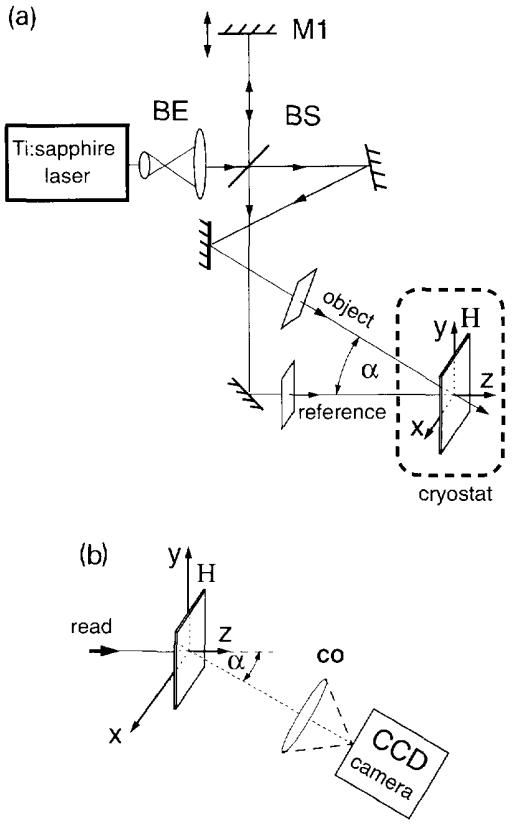

Fig. 1. (a) Scheme of the experimental setup to write the holograms. BE = beam expander; M1 = adjustable delay mirror; BS = beam splitter; H = hologram plane. (b) Optical scheme to observe images in the plane of the hologram. CO = camera objective. (c) Optical scheme to observe Fourier-transformed images. H' = Fourier-transform plane; f = focal length of the cylindrical lens; ξ = Fourier-transform coordinate; MO = microscope objective.

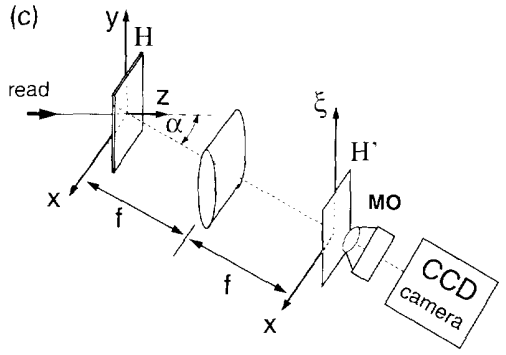

Fig. 1. Continued.

We consider the thickness of the SHB plate to be small compared to the coherence length of the laser pulse. The time it takes for the object wave to illuminate the whole area of the sample is given by,

$$\Delta\tau_{\mathrm{obj}} = \frac{2a\sin\alpha}{c}, \tag{3}$$

where $2a$ is the lateral dimension of the sample in the y-axis direction. If $\tau_0 = 0$, then the two pulses overlap in time at the origin of the coordinates and the width of the overlap region in the y-direction is, $\Delta y \sim \Delta t_p c/\sin\alpha$, where Δt_p is the pulse envelope duration. If $\Delta y \ll 2a$, then in the upper half plane, $a > y > (\Delta t_p c)/2\sin\alpha$, the reference pulse reaches the SHB medium after the object pulse, while in the lower half plane, $-a < y < -\Delta t_p c/2\sin\alpha$, this temporal order is reversed.

The interference between the writing pulses in the hole-burning medium occurs as the first pulse excites the $S_1 \leftarrow S_0$ electronic transition of the molecules, which is then coherently superimposed with the excitation created by the second pulse. The hologram is recorded when photochemical bleaching of the SHB material takes place in a proportion to the intensity of the excitation at a given frequency and at a given spatial location of the material.

Following Ref. [2], the diffraction properties of thin SHB holograms are described by coherent response function,

$$K(\nu, y) \propto (1 + \mathrm{i}\hat{H})\{T_0 + \Delta T(\nu, y)\}, \tag{4}$$

where $\hat{H}$ denotes Hilbert transformation, T_0 is the transmission of the SHB plate before illumination and ΔT is the increase of the transmission due to the writing exposure. In the first approximation, ΔT is proportional to

$$\Delta T(\nu, y) \propto \int_{-\infty}^{\infty} g_0(\nu'')v(\nu - \nu'') \times \left(\int_{-\infty}^{\infty} I(\nu', y)v(\nu' - \nu'')\,\mathrm{d}\nu' \right)\mathrm{d}\nu'', \tag{5}$$

where $v(\nu - \nu')$ is molecule's homogeneous absorption spectrum centered at frequency ν', $g_0(\nu)$ is inhomogeneous distribution function before the exposure, and $I(\nu, y)$ is the frequency and spatial domain distribution of the illumination intensity,

$$I(\nu, y) = |p(\nu - \nu_0)|^2 \left[2 + \mathrm{e}^{\mathrm{i}2\pi\nu\frac{y\sin\alpha}{c}} + \mathrm{e}^{-\mathrm{i}2\pi\nu\frac{y\sin\alpha}{c}} \right], \tag{6}$$

with $p(\nu)$ given by,

$$p(\nu) = \int_{-\infty}^{\infty} p(t')\mathrm{e}^{-\mathrm{i}2\pi\nu t'}\,\mathrm{d}t'. \tag{7}$$

To read out the recorded hologram we illuminate it with a beam which is identical to the writing reference wave. The intensity of the diffracted light is observed in the focal plane of a Fourier-transforming lens which is placed at a focal distance, f, behind the hologram (see Fig. 1(b)). The intensity in the Fourier-transform plane as a function of coordinate ξ, conjugated to the y-coordinate in the hologram plane, and integrated overall frequencies, can be expressed as,

$$I^{\mathrm{FT}}(\xi) \propto \int_{-\infty}^{\infty} \left| \int_{-a}^{a} p(\nu - \nu_0)K(\nu, y)\mathrm{e}^{-\mathrm{i}2\pi\frac{\nu}{c}\frac{\xi y}{f}}\,\mathrm{d}y \right|^2 \mathrm{d}\nu. \tag{8}$$

By substituting Eqs. (4) and (5) into Eq. (8) and by considering only the second term in Eq. (6) which produces signal in the $+1$ diffraction order,

we can rewrite Eq. (8) as,

$$I^{FT}(\xi) \propto g_0 \int_{-\infty}^{\infty} |p(\nu - \nu_0)|^2 \times \left| \int_0^a \int_{-\infty}^{\infty} \int_{-\infty}^{\infty} v(\nu - \nu'') v(\nu' - \nu'') |p(\nu' - \nu_0)|^2 \times e^{i2\pi\left(\nu' \sin\alpha - \nu \frac{\xi}{f}\right)\frac{y}{c}} \, d\nu' \, d\nu'' \, dy \right|^2 d\nu. \quad (9)$$

Here we have for simplicity considered that the inhomogeneous distribution function is constant.

If the homogeneous line shape function consists of only one narrow zero-phonon line, then we can substitute the homogeneous line shape by δ-function and Eq. (9) becomes,

$$I^{FT}(\xi) \propto \int_{-\infty}^{\infty} |p(\nu - \nu_0)|^6 \frac{\left[\sin\frac{\pi\nu a}{c}\left(\sin\alpha - \frac{\xi}{f}\right)\right]^2}{\left[\frac{\pi\nu}{c}\left(\sin\alpha - \frac{\xi}{f}\right)\right]^2} \times d\nu \approx \text{const.} \operatorname{sinc}^2 \frac{\nu_0 a}{c}\left(\sin\alpha - \frac{\xi}{f}\right). \quad (10)$$

We see that the intensity distribution then corresponds to conventional plane wave diffraction on a limited aperture. However, because in our case only half of the response contributes to the $+1$ diffraction order, the width of the aperture is half of the full size of the hologram.

Let us now assume that the aperture of the hologram is large. Then, in the limit, $a \to \infty$, Eq. (9) becomes,

$$I^{FT}(\xi) \propto \int_{-\infty}^{\infty} |p(\nu - \nu_0)|^2 \left| p\left(\nu \frac{\xi}{f \sin\alpha} - \nu_0\right)\right|^4 \times \left| h\left(\nu - \nu \frac{\xi}{f \sin\alpha}\right)\right|^2 d\nu \approx \text{const.} \left| p\left(\nu_0 \frac{\xi}{f \sin\alpha} - \nu_0\right)\right|^4 \times \left| h\left(\nu_0 - \nu_0 \frac{\xi}{f \sin\alpha}\right)\right|^2, \quad (11)$$

where we have introduced the auto-correlation function of the homogeneous absorption profile,

$$h(\nu) = \int_{-\infty}^{\infty} v(\nu') v(\nu + \nu') \, d\nu'. \quad (12)$$

We see that if, in comparison to the homogeneous line shape, the spectrum of the laser pulses can be considered constant, then the spatial intensity distribution (11) is proportional to the square of the auto-correlation function (12). In other words, in the Fourier-transform plane the spatial intensity distribution of the diffracted light gives us directly the homogeneous hole-burning spectrum.

3. Experimental

Our source of ultrashort pulses is a self mode-locked Ti:Sapphire laser (Clark Instrumentation NJA-4) pumped by CW Ar^+-laser (Spectra-Physics BeamLok 2060). The duration of the Ti:Sapphire laser pulses is 70–90 fs at the wavelength of $\lambda \approx 750$ nm and with the spectral width (FWHM) $\Delta\lambda \approx 8$ nm. The repetition rate of the laser is 100 MHz, the average output power is 300 mW.

The experimental set-up is shown in the Fig. 1(a). The laser output is expanded to provide a 2 cm diameter beam with a plane wave front. The beam is divided by a beam splitter into the reference and the object path. The reference beam is applied normal to the hologram plane, while the object beam is forming an angle of $\alpha = 10°$ with the reference path in the y–z plane. The time averaged intensity of the both writing beams at the hologram is 5 mW/cm^2.

By translating the mirror M1 of the reference beam path we adjust the time delay between the two beams to be zero along the horizontal line in the middle of the hologram plane.

The sample is a thin ($\sim 100\,\mu$m) film of 18×22 mm cross-section produced from polyvinylbutyral and doped with molecules of a naphthalocyanine dye (Ciba Geigy HW 807) at a concentration of 10^{-3} mol/l. The sample is mounted in a variable temperature immersion He cryostat. At 2 K the inhomogeneous $S_1 \leftarrow S_0$ absorption band has the maximum at $\lambda = 750$ nm and a width

of 25 nm. The hologram recording exposure is typically 10–30 s. During the read out the illuminating light is attenuated by a factor of 100 with neutral density filters.

Fig. 1(b) shows the optical arrangement to observe the images reproduced in the plane directly behind the hologram. The images are recorded using a near-IR sensitive CCD camera (Sony SSC-M370CE) and a video recorder. The video frames are then digitized and processed by a computer.

Fig. 1(c) shows the optical arrangement to observe Fourier-transformed images. A cylindrical lens with focal length $f = 300$ mm is positioned behind the hologram perpendicular to the path axis of the object beam. The optical electric field amplitude in the focal plane H' is a one-dimensional Fourier transform of the amplitude in the plane H directly behind the hologram, diffracted in the direction of the object beam ($+1$ diffraction order). A microscope objective is used to magnify the image in the Fourier-transform plane.

4. Results and discussion

As the first step in our experiment we study the images recalled directly from the hologram without applying the spatial Fourier transformation. Fig. 2 shows the reconstructed image in the complementary diffraction orders when the CCD camera is sharply focussed in the plane of the sample. The hologram is recorded and read out at the temperature $T = 2$ K. The image (a) is observed in the $+1$ diffraction order when the hologram is illuminated with the reference beam, and the image (b) is observed in the -1 diffraction order when the hologram is illuminated with the object beam. The 1 mm bar shows the actual spatial scale on the hologram and the corresponding delay calculated from Eq. (3) is about 500 fs.

In accord with the causality principle, in the $+1$ diffraction order (a) the signal is observed only in the lower half plane, i.e. when the reference is ahead in time with respect to the object. In the -1 diffraction order (b) the signal is visible only in the upper half plane, i.e. if the time order of the pulses is reversed. These images can be viewed upon as if there is present an opaque screen with a relatively sharp cut-off edge in the plane of the sample. We call this phenomenon 'time edge' to underline that its origin consists in causality-related asymmetry of diffraction of spectrally selective holograms [6].

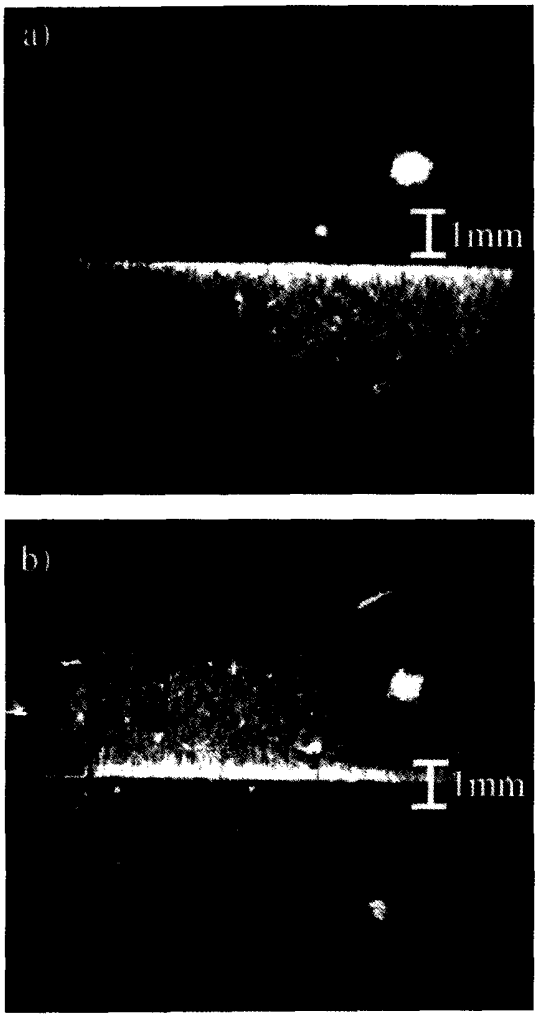

Fig. 2. (a) Image reconstructed from the hologram and recorded with the CCD camera by reading with the reference beam and observing the diffraction in the object beam direction. The recording camera is focussed in the plane of the hologram. (b) Image reconstructed from the same hologram by illumination with the object beam and with the CCD camera placed in the direction of the reference beam. The bars on the left side of the images are used to establish the actual scale of the hologram in the y-axis direction.

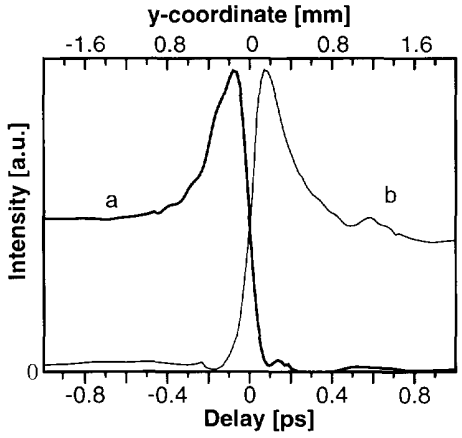

Fig. 3. Intensity distribution in the y-axis direction of the images reconstructed in the two complementary diffraction orders of the hologram. Traces (a) and(b) are obtained from the pictures (a) and (b) in Fig. 2 by integrating in the x-direction and by substraction of the background.

The bright spots in the images are due to lightscattering from imperfections of the sample.

Fig. 3. shows the one-dimensional intensity distributions in the region of the 'time edge' integrated along the x-coordinate. The higher intensity near the 'time edge' arises from the fact that at small delays the interference fringe structure has a larger period in the frequency dimension which means that not only the narrow zero-phonon line, but also the much broader phonon sideband is contributing to the formation of the hologram. We verify this conclusion by comparing the images recorded at different sample temperatures. We observe that at higher temperatures, when the contribution of the phonon side band to the homogeneous spectrum is larger, the relative height of the intensity peak near the 'time edge' increases. At temperatures higher than 77 K essentially only the bright stripe at zero time delay is observed which indicates that the homogeneous spectral width has become comparable to the spectral width of the laser pulses.

It should be noted that in earlier experiments [8, 9] related dependence of the intensity of an incoherently excited accumulated stimulated photon echo signal on the delay between the pump pulses was studied. It was also shown [10–12] that by processing the experimentally measured echo dependences mathematically one can extract information about the homogeneous hole-burning spectrum of the molecules. In contrast to the transient echo methods, in our experiment the variable delay is equivalent to the spatial coordinate, y, and the information about the homogeneous line shape is essentially contained in one holographic image. As we will show below, our experiment allows us to observe the homogeneous line shape directly by purely optical means.

The width of the 'time edge' is in our present experiment approximately $\Delta y \approx 0.1$ mm. When we focus the camera in a plane at some distance behind the hologram, then an intensity pattern of Fresnel diffraction on a sharp edge is observed.

The next step of our experiment is to measure the spatial intensity of the hologram + 1 order signal in the Fourier-transform plane. Figs. 4(a)–(c) show the images in the focal plane of the cylindrical lens magnified by the microscope objective. The three different images correspond to the holograms stored and read out at temperatures 10, 45 and 55 K, respectively. Fig. 4(d) summarizes the corresponding one-dimensional intensity distributions. According to Eq. (11), the spatial scale of the ξ-axis is calibrated in the units of optical frequency, $\xi = 200\,\mathrm{cm}^{-1}/\mathrm{mm}$.

At temperatures below 10 K, when the phonon side band is still very weak compared to the zero-phonon line, the intensity distribution appears in the form of a narrow peak with distinct oscillating side lobes. The width of this peak of $\sim 7\,\mathrm{cm}^{-1}$ is defined by the resolution of our measurement which is inversely proportional to the maximum aperture of the hologram. We attribute this feature to the zero-phonon line in the homogeneous hole-burning spectrum. At temperatures 45 and 55 K the peak intensity of the zero-phonon line is strongly reduced and, at the same time, a broad structure appears on both sides of the central peak. This broad structure extends up to $50\,\mathrm{cm}^{-1}$ and we attribute it to the phonon side band. We can now say that the intensity distribution present in the Fourier-transform plane is nothing else but the homogeneous hole-burning spectrum of our SHB sample.

According to Eq. (11), the spatial intensity distribution has to be symmetric with respect to the

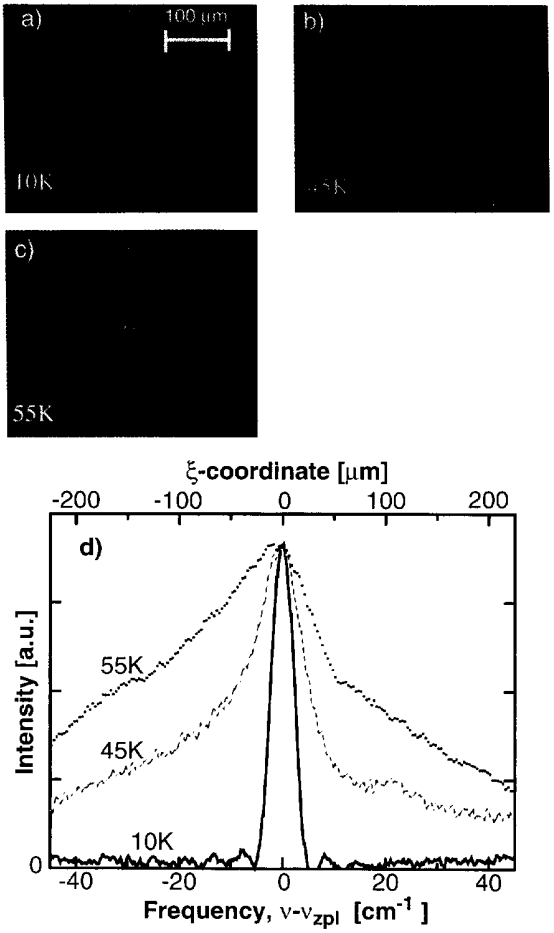

Fig. 4. (a)–(c) Holographic images observed in the focal plane of the Fourier-transforming cylindrical lens at three different sample temperatures. (d) One-dimensional distribution of the corresponding image intensities in the ξ-axis direction. The intensity is integrated along the x-axis.

central peak. The slight asymmetry of the curves in Fig. 4 can be explained either by saturation of the photochemical hole-burning or, which is more probable, by systematic error due to nonuniform illumination intensity of the hologram. The fact that we cannot observe a minimum between the zero-phonon line and the phonon side-band is attributed to the absence of sufficient spectral resolution.

One way to improve the resolution in the present experiment is to increase the effective aperture of the hologram and also to reduce the optical imperfection of the sample. Another interesting further experiment would be to use this setup in the real time regime of two- and three-pulse photon echo. In this case simultaneous frequency and time domain resolution of the coherent response of the molecules could be obtained.

5. Conclusions

We have described a new holographic hole-burning experiment in which optical diffraction on a causality-related virtual 'time edge' is observed. By measuring the intensity profile of the 'time edge' we can obtain information about the homogeneous line shape of the molecules. However, the most intriguing feature of this experiment is that by carrying out spatial Fourier transformation we can observe the homogeneous hole-burning profile directly. In this sense the diffraction on the 'time edge' can be compared to an optical monochromator, although the spectral images we are observing are not directly related to angular dispersion of a grating.

It also follows from our result that if in a four wave mixing type experiment the duration of the pulses becomes small in comparison to the lateral dimensions of the illuminated spot on the sample, then the far field diffraction pattern is directly related to the spectral response of the media. On this basis we believe that further development of this experiment will lead to new methods of time resolved spectroscopy on subpicosecond time scales.

Acknowledgements

We thank H. Spahni and Dr. H. Wolleb (Ciba-Geigy, Marly) for providing the naphthalocyanine compound and Dr. I. Renge for preparing the PVB samples. Support by the Swiss Priority Program 'Optical Sciences, Applications and Technologies' and by KWF (Kommission zur Förderung der Wissenschaftlichen Forschung) is gratefully acknowledged.

References

[1] A. Rebane, R. Kaarli, P. Saari, A. Anijalg, K. Timpmann, Opt. Commun. 47 (1983) 173.
[2] P. Saari, R. Kaarli, A. Rebane, J. Opt. Soc. Am. B 3 (1986) 527.
[3] T.W. Mossberg, Opt. Lett. 7 (1982) 77.
[4] A. Rebane, J. Aaviksoo, J. Kuhl, Appl. Phys. Lett. 54 (1989) 93.
[5] H. Schwoerer, D. Erni, A. Rebane, U. Wild, Opt. Commun. 107 (1994) 123.
[6] A. Rebane, S. Bernet, A. Renn, U.P. Wild, Opt. Commun. 86 (1991) 7; S. Bernet, B. Kohler, A. Rebane, A. Renn, U. P. Wild, JOSA B 9 (1992) 987.
[7] A. Rebane, J. Feinberg, Nature 351 (1991) 378; J. Feinberg, A. Rebane, US Patent 5,313,315 (1994).
[8] S. Asaka, H. Nakatsuka, M. Fujiwara, M. Matsuoka, Phys. Rev. A 29 (1984) 2286.
[9] A.M. Weiner, S. De Silvestri, E.P. Ippen, J. Opt. Soc. Am. B 2 (1985) 654.
[10] S. Saikan, T. Nakabayashi, Y. Kanematsu, N. Tato, Phys. Rev. B 38 (1988) 7777.
[11] J.W-I. Lin, T. Tada, S. Saikan, T. Kushida, T. Tani, Phys. Rev. B 44 (1991) 7356.
[12] R. Kaarli, M. Rätsep, Laser Spectr. 2 (1992) 517.